Journal of Imaging Science and Technology® 52(4): 040908–040908-5, 2008.

Calibrating the Yule–Nielsen Modified Spectral Neugebauer Model with Ink Spreading Curves Derived from Digitized RGB Calibration Patch Images

N. P. Garg, A. K. Singla▲ and R. D. Hersch▲
School of Computer and Communication Sciences, Ecole Polytechnique Fédérale de Lausanne (EPFL), Lausanne, Switzerland
E-mail: rd.hersch@epfl.ch

Abstract. *The Yule–Nielsen modified spectral Neugebauer model (YNSN) enhanced for accounting for ink spreading in the different ink superposition conditions requires a spectrophotometer to measure the reflectances of halftone calibration patches in order to compute the ink spreading curves mapping nominal ink surface coverage to effective ink surface coverage. Instead, as a first step towards the "on the fly" characterization of printers, we try to deduce the ink spreading curves from digitized RGB images of halftone calibration patches. By applying the Yule–Nielsen broadband formula to the average RGB intensities, we deduce the effective dot surface coverages of halftone calibration patches. We then establish the ink spreading curves mapping nominal dot surface coverages to effective dot surface coverages. By weighting the contributions of the different ink spreading curves according to the ratios of colorant surface coverages, we predict according to the YNSN model the reflectance spectra of the test patches. We compare the prediction accuracy of the YNSN model calibrated by digitized RGB intensities of the calibration patches with the prediction accuracy of the same model calibrated by the spectral reflectances of these calibration patches. The decrease in spectral prediction accuracy due to RGB model calibration is about 30% for ink jet prints and 10% for thermal transfer prints. © 2008 Society for Imaging Science and Technology.*
[DOI: 10.2352/J.ImagingSci.Technol.(2008)52:4(040908)]

INTRODUCTION

Many different phenomena influence the reflection spectrum of a color halftone patch printed on a diffusely reflecting substrate (e.g., paper). These phenomena comprise the surface (Fresnel) reflection at the interface between the air and the print, light scattering, and reflection within the substrate (i.e., the paper bulk), and the internal (Fresnel) reflections at the interface between the print and the air. The lateral scattering of light within the paper substrate and the internal reflections at the interface between the print and the air are responsible for what is generally called the optical dot gain, known as the *Yule–Nielsen* effect.

Due to the printing process, the deposited ink dot surface coverage is generally larger than the nominal coverage, yielding a "physical" dot gain responsible for the ink spreading phenomenon.[1] Effective ink dot surface coverages depend on the inks, on the paper, and also on the specific superposition of an ink halftone and other inks. At the present time, according to the literature,[1–3] among the existing spectral reflection prediction models, mainly the well-known Yule–Nielsen modified spectral Neugebauer model[4,5] is used for predicting reflection spectra. This model is further enhanced by accounting for the ink spreading phenomenon.[6] Ink spreading is computed by taking into account the respective physical dot gains of one ink halftone printed in different superposition conditions, i.e., alone on paper, in superposition with one ink, and in superposition with two inks and in superposition with three inks. Effective dot surface coverages are fitted separately for every superposition condition by minimizing a difference metric between measured reflection spectrum and predicted reflection spectrum. This yields, for each superposition condition, an ink spreading curve mapping nominal to effective surface coverages.[6] For spectral prediction of a color halftone, nominal surface coverage values are converted into effective coverage values by weighting the contributions of the different ink spreading curves according to the ratios of colorant surfaces.

In the present contribution, as a first step towards the "on the fly" characterization of printers, we reduce the calibration effort by using digitized RGB images of calibration halftone patches instead of measured reflection spectra. To obtain the ink spreading curves, the unknown effective surface coverage of one ink halftone is calculated according to the broadband Yule–Nielsen formula[4,7–9] an extension of the Murray–Davis formula.[10] The effective surface coverage is deduced from the relation between the mean intensity of a calibration halftone patch and the intensities of patches at 0% and 100% ink surface coverage. After the calibration, the obtained ink spreading curves are used to predict the effective surface coverages of 729 cyan, magenta, and yellow halftone patches. The reflection spectra of the 729 patches are predicted and compared with the measured reflection spectra. We quantify the accuracy of spectral halftone patch predictions by converting measured and predicted spectra first to CIE-XYZ and then to CIE-LAB (Ref. 11, pp. 8–12). The distance defined by the CIE-LAB ΔE_{94} color difference for-

▲IS&T Member.

Received Nov. 26, 2007; accepted for publication Apr. 7, 2008; published online Jul. 17, 2008.
1062-3701/2008/52(4)/040908/5/$20.00.

mula gives a measure of the visually perceived distance between measured and predicted spectra.

INK SPREADING MODEL FOR SPECTRAL REFLECTION PREDICTIONS

The ink spreading model accounting for ink spreading in all ink superposition conditions[6] relies on ink spreading curves mapping nominal surface coverages to effective surface coverages for (a) the surface coverages of single ink halftones, (b) the surface coverages of single ink halftones superposed with one solid ink, and (c) the surface coverage of single ink halftones superposed with two solid inks. In order to obtain the effective coverages (c', m', y') of a color halftone as a function of its nominal surface coverages (c, m, y), the contributions of the different ink spreading curves are weighted according to the ratio of colorants forming that halftone.

During calibration of the model, the ink spreading curves of single ink halftones printed in superposition with paper white, one solid ink or two solid inks are obtained by measuring the reflection spectra $R(\lambda)$ at 25%, 50%, and 75% nominal surface coverages and by fitting effective surface coverages using the Yule–Nielsen modified spectral Neugebauer model (YNSN)[5]:

$$R(\lambda) = \left(\sum_i a_i R_i(\lambda)^{1/n} \right)^n, \tag{1}$$

where a_i is the surface coverage, R_i is the reflection spectrum of ith colorant (also called Neugebauer primary), and n is a scalar coefficient optimized according to the halftone screen frequency ($1 < n < 10$).

By linear interpolation between the obtained effective surface coverages, we obtain the ink spreading curves mapping nominal to effective surface coverages of each ink in each ink superposition condition.

For cyan, magenta, and yellow inks with nominal coverages c, m, and y, the ink spreading functions (curves) mapping nominal coverages to effective coverages for single ink halftones are $f_c(c)$, $f_m(m)$ and $f_y(y)$. The functions mapping nominal coverages of an ink to effective coverages of that ink, for single ink halftones superposed with a second solid ink and for single ink halftones superposed with two solid inks are $f_{c/m}(c)$, $f_{c/y}(c)$, $f_{m/c}(m)$, $f_{m/y}(m)$, $f_{y/c}(y)$, $f_{y/m}(y)$, $f_{c/my}(c)$, $f_{m/cy}(m)$, $f_{y/cm}(y)$, where $f_{i/j}(i)$ indicates an ink halftone i superposed on solid ink j, and where $f_{i/jk}(i)$ indicates an ink halftone i superposed on solid inks j and k.

In the case of three inks, these 12 functions may, for example, be obtained by fitting 36 patches, i.e., three patches (25%, 50%, and 75% nominal coverages) per function. In order to obtain the effective surface coverages c', m' and y' of a color halftone patch, it is necessary, for each ink, to weight the contributions of the corresponding ink spreading curves. For example for cyan ink, we need to weight the contributions of the curves f_c, $f_{c/m}$, $f_{c/y}$, and $f_{c/my}$. The weighting functions depend on the effective surface coverages of the colorants on which the considered ink halftone is superposed. Let us assume that inks are printed independently of each other. For the considered system of 3 inks *cyan*, *magenta and yellow* with nominal coverages c, m and y and effective coverages c', m' and y', the Eqs. (2) are obtained by computing the relative weight, i.e., the relative surface of each underlying colorant.

In analogy with Demichel's Eqs. (3),[12] the relative weight of the cyan colorant (*cyan* on top of *paper*) is $(1-m')\ (1-y')$, the blue colorant (*cyan* on top of colorant *magenta)* is $m'\ (1-y')$, the green colorant (*cyan* superposed with colorant *yellow)* is $(1-m')\ y'$ and the black colorant (*cyan* superposed with solid *magenta* and *yellow)* is $m'y'$. The resulting system of equations is[6]

$$\begin{aligned}
c' &= f_c(c)(1-m')(1-y') + f_{c/m}(c)m'(1-y') \\
&\quad + f_{c/y}(c)(1-m')y' + f_{c/my}(c)m'y' \\
m' &= f_m(m)(1-c')(1-y') + f_{m/c}(m)c'(1-y') \\
&\quad + f_{m/y}(m)(1-c')y' + f_{m/cy}(m)c'y' \\
y' &= f_y(y)(1-c')(1-m') + f_{y/c}(y)c'(1-m') \\
&\quad + f_{y/m}(y)(1-c')m' + f_{y/cm}(y)c'm'
\end{aligned} \tag{2}$$

This system of equations can be solved iteratively: one starts by setting initial values of c', m', and y' equal to the respective nominal coverages c, m, and y. After one iteration, one obtains new values for c', m', and y'. These new values are used for the next iteration. After a few iterations, typically 4–5 iterations, the system stabilizes and the obtained coverages c', m' and y', are the effective coverages. The system of Eqs. (2) yields the effective surface coverages of cyan, magenta, and yellow inks for the corresponding nominal surface coverages.

The effective colorant coverages are obtained from the effective coverages of the inks according to the Demichel Eqs. (3) which give the respective surface coverages of the colorants as a function of the surface coverages of the individual inks. In case of independently printed cyan, magenta, and yellow inks of respective surface coverages c', m', y', the respective fractional areas of the colorants white, cyan, magenta, yellow, red (superposition of magenta and yellow), green (superposition of yellow and cyan), blue (superposition of magenta and cyan), and black (superposition of cyan, magenta and yellow) are

$$\begin{aligned}
&\text{white:} && a'_w = (1-c')(1-m')(1-y') \\
&\text{cyan:} && a'_c = c'(1-m')(1-y') \\
&\text{magenta:} && a'_m = (1-c')m'(1-y') \\
&\text{yellow:} && a'_y = (1-c')(1-m')y' \\
&\text{red:} && a'_r = (1-c')m'y' \\
&\text{green:} && a'_g = c'(1-m')y' \\
&\text{blue:} && a'_b = c'm'(1-y') \\
&\text{chromatic black:} && a'_k = c'm'y'
\end{aligned} \tag{3}$$

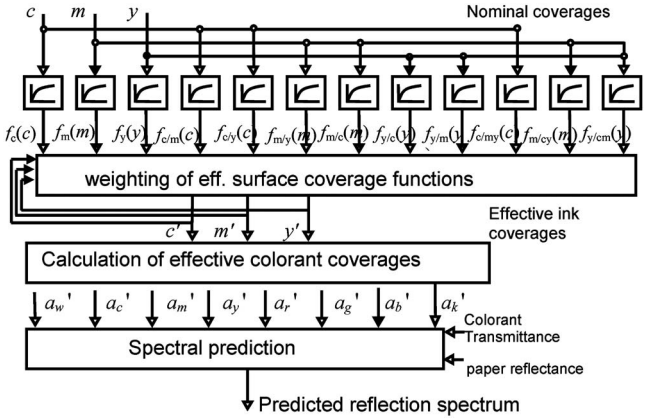

Figure 1. Spectral prediction model with ink spreading in all superposition conditions.

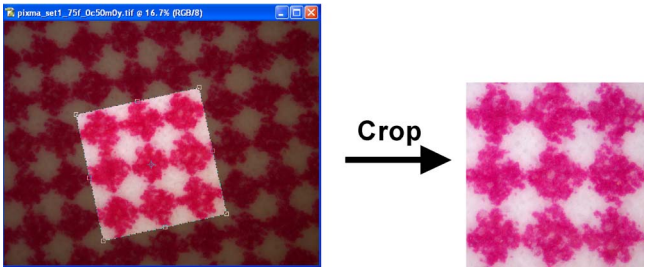

Figure 2. Cropping of a halftone image acquired with a microscope.

The complete model accounting for ink spreading in all superposition conditions is illustrated in Figure 1. The n-value of the Yule–Nielsen modified spectral Neugebauer model for a given printer and screen element frequency is obtained by computing for a subset of the considered color samples the mean CIELAB ΔE_{94} color difference between predicted and measured reflection spectra. By iterating across possible n values, one selects the n value yielding the lowest color difference between predicted and measured reflection spectra.

INK SPREADING CURVES RELYING ON DIGITIZED RGB INTENSITIES

We would like to facilitate the acquisition of the ink spreading curves mapping nominal to effective surface coverages by using digitized RGB images of halftone patches. The RGB images may be digitized with a camera hooked on a microscope or with a scanner, in reflectance mode.

The microscopic images are acquired according to a 45°/0° geometry, i.e., a circular light source illuminates the sample dot at 45° and the image is captured normal to the print surface. This avoids capturing the specular reflection. Since the microscope enlarges the halftone dots, it is important to ensure that the halftone surface coverage in the digitized image is the same as within the actual halftone patch. We therefore crop a periodic array of halftone dots from patches acquired with the microscope (Figure 2). The size w

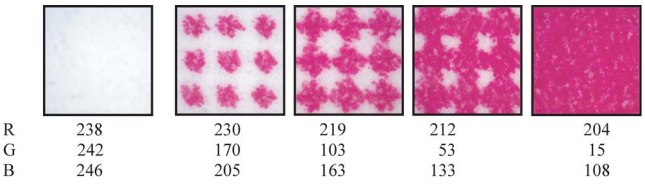

Figure 3. Mean intensities of the R, G, and B channels of calibration halftone patches digitized by a camera hooked onto a microscope (max value: 255), with 0%, 25%, 50%, 75% and 100% nominal surface coverages of magenta ink on paper.

in pixels of the cropped square image can be calculated according to the magnification of the microscope M, the screen frequency f, and the resolution r of the acquired microscope image

$$w = (\mu/f)rM, \tag{4}$$

where μ is the number of halftone dots we wish to have in the cropped image.

In the case of halftone images acquired by a scanner it is not necessary to crop a periodic pattern because the scanned halftone image covers a larger area over which the exact placement of the cropping window has a negligible influence.

After acquiring and processing the camera images, calibration is carried out by deriving from the mean intensity of the image the effective surface coverages of the inks. We consider the color channel where the ink halftone has the greatest absorption. The cyan ink absorbs in the red wavelength range, the magenta ink absorbs in the green wavelength range, and the yellow ink absorbs in the blue wavelength. For example, when we vary the amount of magenta ink on paper, on one solid ink or on two solid inks, the intensity of the green image channel is the most affected (Figure 3).

With the normalized intensity of the corresponding channel, we calculate the effective surface coverage for 25%, 50%, and 75% nominal surface coverages according to the Yule–Nielsen broadband formula[7–9]

$$u' = \frac{(I_0)^{\gamma/n_{\mathrm{RGB}}} - (I_u)^{\gamma/n_{\mathrm{RGB}}}}{(I_0)^{\gamma/n_{\mathrm{RGB}}} - (I_{100})^{\gamma/n_{\mathrm{RGB}}}}, \tag{5}$$

where u' is the effective surface coverage when the nominal surface coverage of the considered ink halftone is u, and I_u, I_0, I_{100} are the normalized mean intensities at respectively a nominal surface coverage of u, 0% and 100%. The scalar variable n_{RGB} is the n value of the Yule–Nielsen broadband formula and γ is the gamma value that the acquisition device uses internally for transforming sampled linear RGB values into nonlinear gamma corrected R′G′B′ values. A value of $\gamma = 2.2$ is generally used in commercial scanners.[13,14]

By carrying out this calculation for patches of one ink at nominal coverages of 25%, 50%, and 75% printed either on paper alone or superposed with one solid ink, respectively two solid inks, one obtains by linear interpolation the ink spreading curves mapping nominal to effective surface cov-

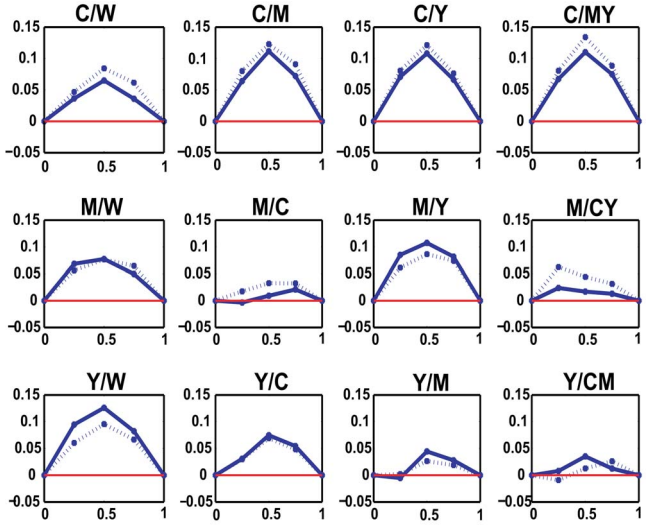

Figure 4. Dot gain curves associated with ink spreading curves in the different superposition conditions, with effective surface coverages computed from digitized RGB images (continuous) and from spectral YNSN model fits (dotted), for thermal transfer prints at a screen frequency of 75 lpi and a resolution of 600 dpi.

erage in all superposition conditions. Figure 4 shows the ink spreading dot gain functions, defined as effective surface coverages minus nominal surface coverages.

The correctness of the obtained ink spreading curves is verified by using them within the YNSN model to predict the reflection spectra of the 729 test patches. The predicted reflection spectra are compared with the measured reflection spectra by applying the CIELAB ΔE_{94} color difference formula, which gives a measure of the spectral prediction accuracy (see Tables I and II).

Regarding the n values, one ratio γ/n_{RGB} is used for computing the ink spreading curves with the Yule–Nielsen broadband expression (5) and a second n value (n_s) is used for predicting the spectra of the test patches from their nominal surface coverages according to the YNSN model, Eq. (1). Since the n value reflects the optical dot gain, a separate n value is required for the Yule–Nielsen broadband model with patches digitized by a camera hooked on a microscope or by a scanner.

The broadband model ratio γ/n_{RGB} and the spectral prediction model n value are obtained during a first calibration and test of the model by minimizing for a subset of the considered color samples the mean CIELAB ΔE_{94} color difference between predicted and measured reflection spectra.

Once the acquisition device's ratio γ/n_{RGB} and the YNSN model n value are known, we need only the reflectance spectra of the eight colorants and the digital images of the 44 calibration patches for the calibration of the model. The digital images can be acquired by an automated process.

RESULTS

We carried out spectral predictions with the ink spreading curves calibrated by relying on RGB images of cyan, magenta, and yellow patches. The experiments were performed on a thermal transfer wax printer (OKI DP-7000, 600 dpi, calendered paper) and on an ink jet printer (Canon PIXMA 4000 at 600 dpi, coated paper) at screen frequencies of 75 lpi and 100 lpi. Tables I and II give the mean prediction errors in terms of ΔE_{94} values, the maximal prediction error, and the number of patches having a prediction error larger than $\Delta E_{94}=3$. For calculating the ink spreading curves, only 25%, 50%, and 75% nominal coverages are used in each superposition condition. This yields $3\times12=36$ calibration patches.

In addition, for the broadband Yule–Nielsen Eq. (5), we need the digitized RGB images of the paper white, the solid inks, and all the solid ink superpositions (for three inks: eight patches). The model is tested on 729 patches comprising all nominal surface coverage combinations of 0%, 13%, 25%, 38%, 50%, 63%, 75%, 88%, and 100%. For comparison, we present the prediction accuracies with the calibration of the ink spreading curves performed by spectral fits according to the YNSN model, for the same printing devices, same paper, same ink, and same screen frequency as above. In addition, as a reference we consider also a single ink

Table I. Prediction accuracies for ink jet prints.

Ink jet prints (Canon Pixma 4000)	Classical halftone screen				
	n		Mean	Max	No. samples
729 test samples	n_s	n_{RGB}	ΔE_{94}	ΔE_{94}	$\Delta E_{94}>3$
Predictions using spectral data (75 lpi)					
Single ink dot-gain only	4.0		2.87	9.36	283
Ink spreading in all superimposition conditions	3.8		1.00	2.37	0
Predictions using image data (75 lpi)					
Ink spreading in all superimposition conditions (microscope, unknown γ)	3.6		1.33	5.64	13
Ink spreading in all superimposition conditions (scanner, $\gamma=2.2$)	2.5	3	1.29	3.52	11
Predictions using spectral data (100 lpi)					
Single ink dot-gain only	18.0		3.18	8.65	346
Ink spreading in all superimposition conditions	6.7		0.98	2.58	0
Predictions using image data (100 lpi)					
Ink spreading in all superimposition conditions (microscope, unknown γ)	6.7		1.40	4.24	4
Ink spreading in all superimposition conditions (scanner, $\gamma=2.2$)	3.6	3.3	1.38	4.94	35

Table II. Prediction accuracies for thermal transfer prints.

Thermal transfer prints (Oki 7000)	Classical halftone screen				
	n		Mean	Max	No. samples
729 test samples	n_s	n_{RGB}	ΔE_{94}	ΔE_{94}	$\Delta E_{94} > 3$
Predictions using spectral data (75 lpi)					
Single ink dot-gain only	2.4		1.57	4.23	17
Ink spreading in all superimposition conditions	1.4		1.22	4.80	22
Predictions using image data (75 lpi)					
Ink spreading in all superimposition conditions (scanner, $\gamma = 2.2$)	1.5	2.2	1.36	3.90	15
Predictions using spectral data (100 lpi)					
Single ink dot-gain only	2.7		1.93	5.29	63
Ink spreading in all superimposition conditions	1.7		1.37	3.88	15
Predictions using image data (100 lpi)					
Ink spreading in all superimposition conditions (scanner, $\gamma = 2.2$)	1.5	2.2	1.45	4.62	16

spreading function per ink obtained by computing the effective surface coverages of single ink halftones printed on paper, noted *single ink dot gain only*.[1]

The prediction results shown in the Tables clearly demonstrate that the full ink spreading model deduced from RGB images yields a much better prediction accuracy than the classical single ink dot gain relying on spectral fits. The full ink spreading model relying on digitized RGB images offers a slightly lower accuracy compared with the one calibrated with measured reflection spectra.

For ink jet prints, the tests were performed both on the images digitized by a camera hooked onto a microscope as well as on the images acquired by the scanner. Scanner acquisition and microscope acquisition provide the same accuracy. However, scanner acquisition is much easier to perform and can be automated.

CONCLUSIONS

We reduce the effort of calibrating the Yule–Nielsen modified spectral Neugebauer model accounting for full ink spreading by computing the nominal to effective surface coverage curves from digitized RGB images instead of from measured reflection spectra. For the calibration of the model by digitized RGB images, we need to measure only the reflection spectra of the solid colorant patches (for three inks: eight patches) and digitize one sheet containing all calibration patches (for three inks, 44 patches).

By using images instead of spectra, the prediction accuracy is not much affected. Tests were carried out with 729 color patches covering the complete gamut of the output device. In case of cyan, magenta, and yellow ink jets prints at 75 lpi, the mean ΔE_{94} difference between predicted and measured reflection spectra for calibration by spectral fits was 1.00. When calibrating with digitized RGB images, the mean prediction difference is $\Delta E_{94} = 1.29$. For thermal transfer prints, the mean ΔE_{94} difference between predicted and measured reflection spectra using spectrally fitted ink spreading curves was 1.22 and 1.36 when using ink spreading curves deduced from scanned images.

Further work is required for extending the spectral prediction model relying on RGB images to four inks, i.e., cyan, magenta, yellow, and black inks. This is difficult because one cannot easily distinguish between pure black and the chromatic black obtained by superimposing similar amounts of cyan, magenta, and yellow.[15]

REFERENCES

[1] R. Balasubramanian, "Optimization of the spectral Neugebauer model for printer characterization", J. Electron. Imaging **8**, 156–166 (1999).
[2] D. R. Wyble and R. S. Berns, "Add critical review of spectral models applied to binary color printing", Color Res. Appl. **25**, 4–19 (2000).
[3] T. Ogasahara, "Verification of the predicting model and characteristics of dye-based ink jet printer", J. Imaging Sci. Technol. **48**, 130–137 (2004).
[4] J. A. C. Yule and W. J. Nielsen, "The penetration of light into paper and its effect on halftone reproductions", *Proc. TAGA Conference 1951* (TAGA, Sewickley, PA) pp. 65–76.
[5] J. A. S Viggiano, "Modeling the color of multi-colored halftones", *Proc. TAGA Conference 1990* (TAGA, Sewickley, PA) pp. 44–62.
[6] R. D. Hersch and F. Crété, "Improving the Yule–Nielsen modified spectral Neugebauer model by dot surface coverages depending on the ink superposition conditions", Proc. SPIE **5667**, 434–445 (2005).
[7] J. A. S Viggiano, "The color of halftone tints", *Proc. TAGA Conference 1985* (TAGA, Sewickley, PA) pp. 647–661.
[8] I. Pobborovsky and M. Pearson, "Computation of dot areas required to match a colorimetrically specified color using the modified Neugebauer equations", *Proc. TAGA Conference 1972* (TAGA, Sewickley, PA) pp. 65–77.
[9] J. S. Arney, P. G. Engeldrum, and H. Zeng, "An expanded Murray-Davis model of tone reproduction in halftone imaging", J. Imaging Sci. Technol. **39**, 502–508 (1995).
[10] A. Murray, "Monochrome reproduction in photoengraving", J. Franklin Inst. **221**, 721–724 (1936).
[11] H. R. Kang, *Color Technology for Electronic Imaging Devices* (SPIE Optical Engineering Press, Bellingham, WA, 1997).
[12] M. E. Demichel, Procédé **26**, 17–21 (1924).
[13] K. Parulski and K. Spaulding, "Color image processing for digital cameras", in *Digital Color Imaging Handbook*, edited by G. Sharma (CRC, Boca Raton, FL, 2003), Chap. 12, pp. 744–748.
[14] C. Poynton, "Color Science and Color Appearance Models", SIGGRAPH 2004 Course notes, available at www.poynton.com.
[15] T. Bugnon, M. Brichon, and R. D. Hersch, "Model-based deduction of CMYK surface coverages from visible and infrared spectral measurements of halftone prints", Proc. SPIE **6493**, 649310-1-10 (2007).